A Twining Company

2800 Wilderness Place Suite A
Boulder, CO 80301
T: 303.938.0166
www.drpcinc.com

Petrographic Investigation of A Concrete Core Extracted from the Backwall of the US 89 Bridge Over Belt Creek

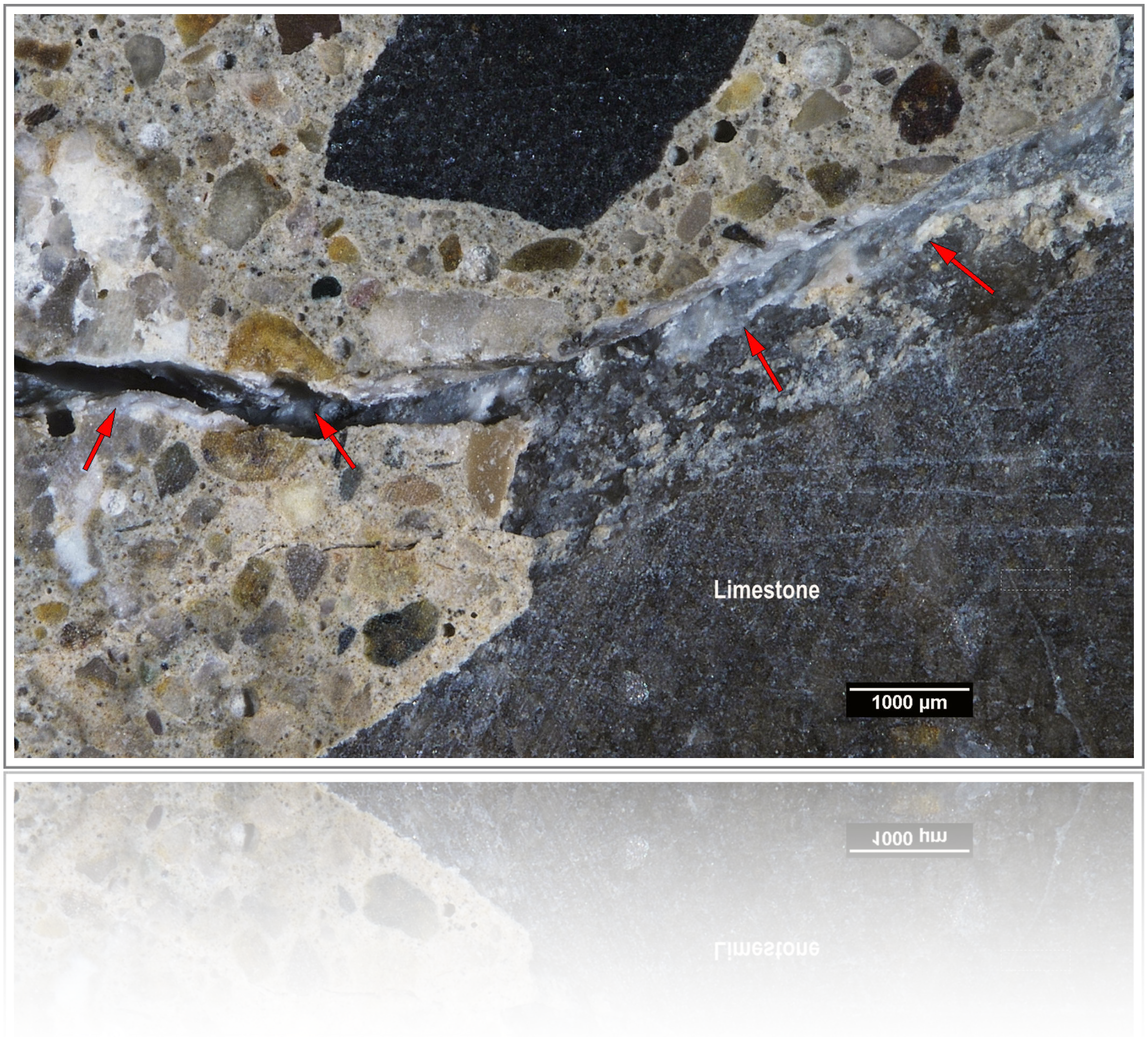

Prepared for Michael Berry, Ph.D.
Montana State University
Bozeman, Montana

Prepared by David Rothstein, Ph.D., P.G., FACI
Report No. 217649.d
2 June 2021

EXECUTIVE SUMMARY

A core extracted from the backwall of a US Highway 89 bridge over Belt Creek in Montana is the subject of petrographic examination. The purpose of the examination is to characterize the composition and condition of the concrete represented by the core and to determine if there is evidence of damage associated with any durability mechanism(s) such as alkali-silica reaction (ASR).

The findings from this scope of work indicate that the concrete shows moderate to severe damage from ASR based on a qualitative scale from DRP. The progression of the reaction is at Stage IV of six stages using the scale of Katayama [**1**]. The ASR involves siliceous limestone, quartzite and granitic rocks in the coarse and fine aggregate.

The composition of the concrete is as follows. The paste contains hydrated portland cement with no fly ash or other supplemental cementitious materials observed. The concrete is marginally air-entrained with 3-4% total estimated air. The coarse aggregate is a natural gravel with a 50 mm (2 in.) nominal top size although most particles are less than 19 mm (¾ in.) across. The aggregate consists of siliceous and carbonate rocks that include limestone, siliceous limestone, quartzite,, chert and siliceous volcanic rocks. The fine aggregate is a natural sand that consists of rocks similar to those in the coarse aggregate.

1 Leeman, A. and Katayama, T., 2020, Introduction to Diagnosis, *in Diagnosis & Prognosis of AAR Affected Structures,* State-of-the-Art Report of the RILEM Technical Committee 259-ISR

1.0 INTRODUCTION

Professor Michael Berry, Ph.D. of the Civil Engineering Department at Montana State University (**MSU)** located in Bozeman, Montana requested DRP, a Twining Company (**DRP**) to perform a petrographic examination on a concrete core extracted from the backwall of a US Highway 89 bridge over Belt Creek in Montana. The purpose of the examination is to characterize the composition and condition of the concrete represented by the core and to determine if there is evidence of damage associated with any durability mechanism(s) such as alkali-silica reaction (ASR).

On 12 May 2021 **DRP** received two (2) concrete cores from **MSU**. The cores were labeled as #2 and #3 and assigned **DRP** numbers 25YD11241 and 25YD11242, respectively. No information was provided regarding the age of the concrete, the original concrete mix design or any information regarding independent material tests conducted during or after the construction of the bridge. Dr. Berry provided several photographs showing cracks and white exudations on the backwall from which the cores were extracted. The cores were reportedly taken adjacent to each other such that they represent essentially the same concrete. Core #3 was selected for the present analysis.

2.0 SCOPE OF WORK

The testing involved petrographic examination according to ASTM C856 [**2**]. Air content was estimated based on visual and microscopical observations but not measured per ASTM C457 [**3**].

Appendix A contains the notes, photographs and micrographs from the petrographic examinations, and *Appendix B* describes the procedures used to perform this scope of work. The petrographic work was performed by a chief scientist and reviewed by the principal petrographer.

2 *Standard Practice for Petrographic Examination of Hardened Concrete.* Annual Book of ASTM Standards, Vol. 4.02., ASTM C856-18.

3 *Standard Test Method for Microscopical Determination of Parameters of the Air-Void System in Hardened Concrete*, Annual Book of ASTM Standards, Vol. 4.02, ASTM C457-16.

ASR Ranking **DRP** rates the severity of damage associated with ASR and the stage of the reactions associated with ASR using two different schemes. The first is a qualitative ranking developed by DRP that describes the severity of damage (**Table 1)**. The second is a petrographic description of the stages of ASR based on criteria developed by Katayama ([**1**].; **Table 2**).

Table 1. DRP criteria for severity of ASR damage

Severity	Criteria
Absent	No reaction rims, microcracks or cracks associated with ASR
Negligible	Only reaction rims observed
Trace	ASR gel rarely observed lining voids near aggregate particles
Minor	ASR gel in voids near reactive particles or rimming reactive particles; microcracks with ASR gel rarely to occasionally observed
Moderate	Microcracks commonly filled with ASR gel commonly observed
Severe	Cracks (> 100 µm wide) filled with ASR gel observed

Table 2. Petrographic stages of ASR (after [1])

Stage	Criteria
I	Formation of reaction rims within aggregate particles.
II	Halo of ASR sol/gel around aggregate particles. Darkening of paste around aggregate particles.
III	Cracking of aggregate; ASR gel may line or fill crack.
IV	Propagation of cracks from reacted aggregate into paste. ASR gel may line or fill crack; crack width grows.
V	Gel fills voids along cracks distal to aggregate particles.
VI	Development of gel-filled cracks between aggregate particles.

3.0 Findings

The following observations are relevant to the concrete represented by the sample. The figures referenced herein are in *Appendix A.*

- The core is horizontal in orientation and measures ~ 95 mm (3 ¾ in.) in diameter (**Figure A1**, **Figure A2**). The outer surface is formed and the inner surface is a fracture, such that the core represents a partial thickness of the backwall (**Figure A3**). White secondary deposits consisting of ASR gel were observed on the inner fracture surface (**Figure A4**).
- No steel reinforcement of other embedded objects were observed.
- Linear cracks up to 250 µm (10 mil) were observed on the outer surface that cut sub-horizontally up to 30 mm (1 ⅛ in.) into the core (**Figure A5**). Deposits of gel were observed along segments of the cracks (**Figure A6**). Microcracks ranging from 25-75 µm (1-3 mil) wide were observed over the full depth of the core. The microcracks typically radiate from reactive aggregate particles and contain deposits of ASR gel (**Figure A7**).
- The paste is gray in and moderately hard (Mohs ~ 3.0) with a smooth texture and sub-vitreous luster (**Figure A8**). A fresh fracture surface cuts mostly through aggregate particles and shows deposits of ASR gel (**Figure A9**). The paste contains portland cement with no fly ash, slag cement or other supplemental cementitious materials observed; the hydration is normal (**Figure A10**). The capillary porosity of the paste is moderate and the estimated w/c is 0.45 ± 0.05 (**Figure A11**).
- The coarse aggregate is a natural gravel that has a 50 mm (2 in.) nominal top size but most particles are 19 mm (¾ in.) or less (**Figure A12**). The aggregate is a mixture of carbonate and siliceous rocks that include limestone, quartzite, granitic rocks, chert and siliceous volcanic rocks. Some of the limestones are siliceous. The fine aggregate is a natural sand that consists of rock types similar to those observed in the coarse aggregate (**Figure A13**). Evidence of ASR was observed involving siliceous limestone, granitic rocks and quartzites (which contain class of chert) in the coarse and fine aggregate.
- The concrete is marginally air-entrained with 3-4% total estimated air content (**Figure A14**). The concrete is well consolidated with no major water voids or consolidation voids observed.
- Secondary deposits consists of calcium carbonate, ettringite and ASR gel. Carbonation was observed for up to 15 mm (⅝ in.) from the outer surface (**Figure A15**). Deposits of ettringite were occasionally observed in voids inboard of the carbonated zone (**Figure A16**). SDeposits of ASR gel were observed in voids, cracks and microcracks and around aggregate particles (**Figure A5-Figure A7; Figure A17**). The core shows it is in Stage IV using the qualitative scale of Katayama [**1**] with moderate to severe damage from ASR using the DRP scale. The ASR primarily involves limestone, quartzite and granitic rocks in the coarse and fine aggregate.

This concludes work performed on this project to date.

David Rothstein, Ph.D., P.G., FACI
Principal Petrographer

US 89 Over Belt Creek Backwall Core Petrography

Appendices

1. Received Condition	
Orientation & Dimensions	Horizontal core from bridge backwall measures ~ 95 mm (3 ¾ in.) in diameter and 65-85 mm (2 ½-3 ⅜ in.) in length (**Figure A1, Figure A2**).
Surfaces	The outer surface is formed and the inner surface is a fracture such that the core represents a partial thickness of the backwall (**Figure A3**). The inner surface cuts through aggregate particles; white secondary deposits observed commonly rimming aggregate particles (**Figure A4**).
General Condition	The core is hard and compact. Several cracks observed on outer surface that range from hairline (~ 100 µm or 4 mil wide) to 250 µm (10 mil) wide. The cracks are mostly linear with several triple points observed. White secondary deposits observed on outer surface.

2. Embedded Objects	
General	None observed.

3. Cracking	
Macroscopic	Linear cracks ranging from hairline to 250 µm (10 mil) wide observed on outer surface (**Figure A5**). Cracks cut mostly sub-horizontally up to 30 mm (1 1/8 in.) on the side of the core. On the polished slab cracks up to 250 µm (10 mil) wide cut through the full length of the core. The cracks cut mostly around but occasionally through aggregate particles. The cracks occasionally show bifurcations into smaller hairline cracks and microcracks. Deposits of ASR gel were observed along the walls of the cracks in distinct segments of their strike length (**Figure A6**).
Microscopic	Microcracks observed occasionally over the full depth of the core; the microcracks are mostly 25-75 µm (1-3 mil) wide and up to 6 mm (1/4 in.) long (**Figure A7**). These microcracks radiate from aggregate particles and contain deposits of ASR gel.

4. Paste Observations	
Polished Surface	The paste is gray (Munsell 2.5Y/5/1) except in the outer 1-2 mm (40-80 mil) where the paste is dark gray (2.5Y/4/1) and from 15-19 mm (⅝-¾ in.) where the paste is light brown (2.5Y/7/3; **Figure A8**). The paste is moderately hard (Mohs ~ 3.5) and has a smooth texture and sub-vitreous luster.
Fracture Surface	Fresh fracture is gray and has a semi-hackle texture (**Figure A9**). The fracture cuts through > 75% of coarse aggregate particles. Deposits of ASR gel and ettringite were observed.
Thin Section	The paste contains hydrated portland cement; no fly ash, slag cement or other SCM were observed. The hydration of the paste is normal to advanced. The hydrated paste contains 4-8% RRCG that consist primarily of belite grains with interstitial aluminoferrite; alite was rarely observed and is very fine-grained with hydration rims (**Figure A10**). CH is medium-grained and evenly distributed and makes up 8-15% of the paste.
Estimated w/cm	The capillary porosity of the majority of the paste is moderate and moderately heterogeneous (**Figure A11**). The estimated w/cm is 0.45±0.05.

** Abbreviations as follows: DSL = densified surface layer; RRCG = relict and residual cement grains; SCM = supplemental cementitious materials; CH = calcium hydroxide; ITZ = interfacial transition zone. Modal abundances are based on visual estimations.*

5. Coarse Aggregate	
Physical Properties	The coarse aggregate is a natural gravel with a 50 mm (2 in.) nominal top size but most particles are 19 mm (¾ in.) or less across (**Figure A12**). The rocks are hard and compact. The particles are sub-equant to slightly elongated in shape with well-rounded to sub-rounded edges. The limited length of the core precludes discussion of grading and distribution.
Rock Types	The coarse aggregate is a mixture of carbonate and siliceous rocks that are mostly sedimentary and igneous in origin. Major rock types include limestone, quartzite, granitic rocks and siliceous volcanic rocks such as rhyolite. The limestones range from massive micritic rocks to sandy limestones. None of the limestone shows evidence of significant dolomitization and none of them contain argillaceous seams or have textures commonly associated with rocks that are potentially susceptible to alkali-carbonate reaction (ACR). Quartzite, granitic rocks and siliceous volcanic rocks are potentially susceptible to alkali-silica reaction (ASR).
Other Features	No ACR is observed. No deleterious coatings or encrustations were observed. No low w/c mortar coatings were observed. Evidence of ASR was observed with deposits of ASR gel lining walls of cracks and lining and filling occasional air voids. The reactive components include granitic rocks and quartzite in the coarse aggregate.

6. Fine Aggregate	
Physical Properties	The fine aggregate is a natural sand that consists of particles that are hard and compact. The particles are mostly sub-equant in shape with sub-angular to sub-rounded edges. The grading and distribution is relatively even (**Figure A13**).
Rock Types	The fine consists of a mixture of rock types similar to those observed in the coarse aggregate.
Other Features	Evidence of ASR involving granitic rocks and quartzite in the sand was observed. No deleterious coatings or encrustations were observed. No low w/c mortar coatings were observed. No evidence of ACR observed.

7.Voids	
Void System	The concrete is marginally air-entrained with 3-4% total estimated air content (**Figure A14**). No significant water voids or consolidation voids were observed.
Void Fillings	Voids commonly contain deposits of ettringite and occasionally contain deposits of ASR gel.

8. Secondary Deposits	
Phenolphthalein	No staining for up to 15 mm (⅝ in.) from the outer surface (**Figure A15**).
Secondary Deposits	Deposits include pervasive carbonation in the outer 15 mm (⅝ in.), deposits of ettringite in air voids inboard of the carbonated zone (**Figure A16)** and deposits of ASR gel in microcracks, air voids and rimming aggregate particles (**Figure A17**).

FIGURES

(a)

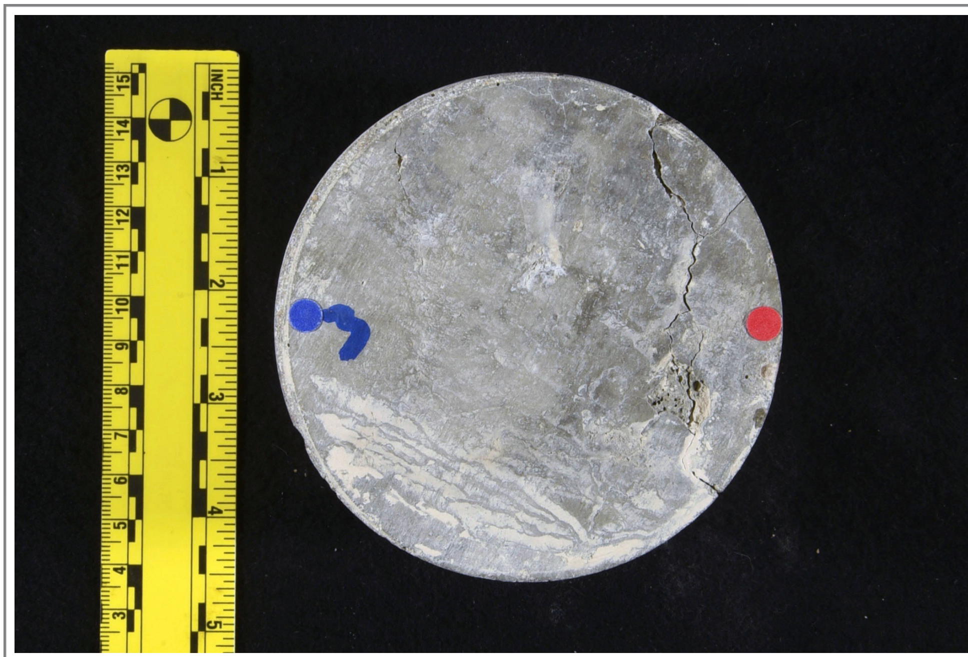

(b)

Figure A1. Photographs of the core in as-received condition showing (a) an oblique view of the outer surface and side of the core with identification labels and (b) the outer surface of the core. The red and blue dots show the orientation of the saw cuts used to prepare the core. The small and large divisions are in centimeters and inches, respectively.

(c)

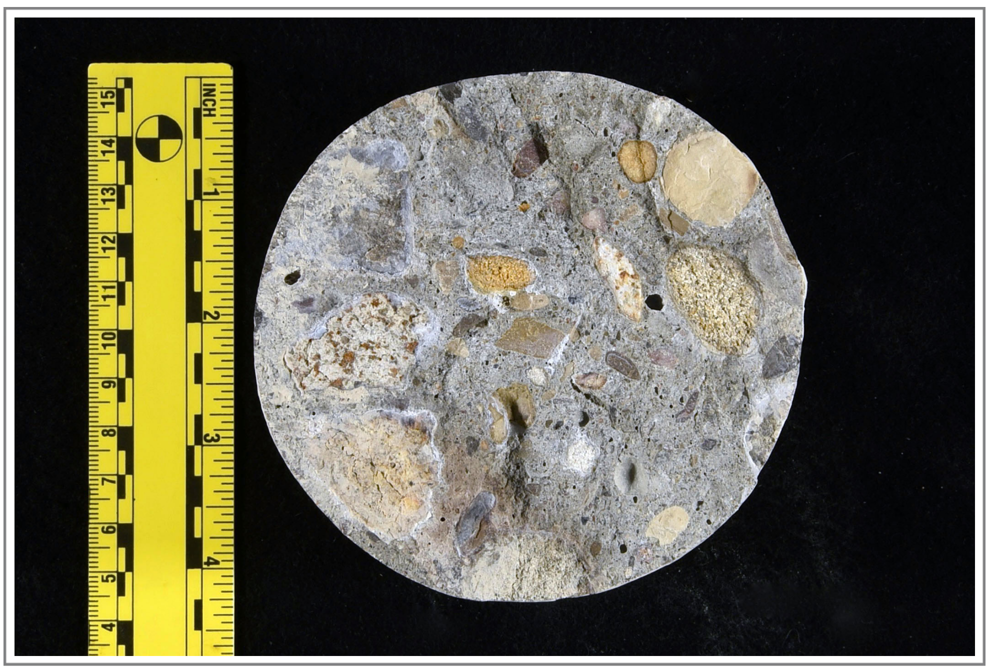

(d)

Figure A1 (cont'd). Photographs of the core in as-received condition showing (c) the side of the core and (d) the inner surface of the core. The small and large divisions are in centimeters and inches, respectively.

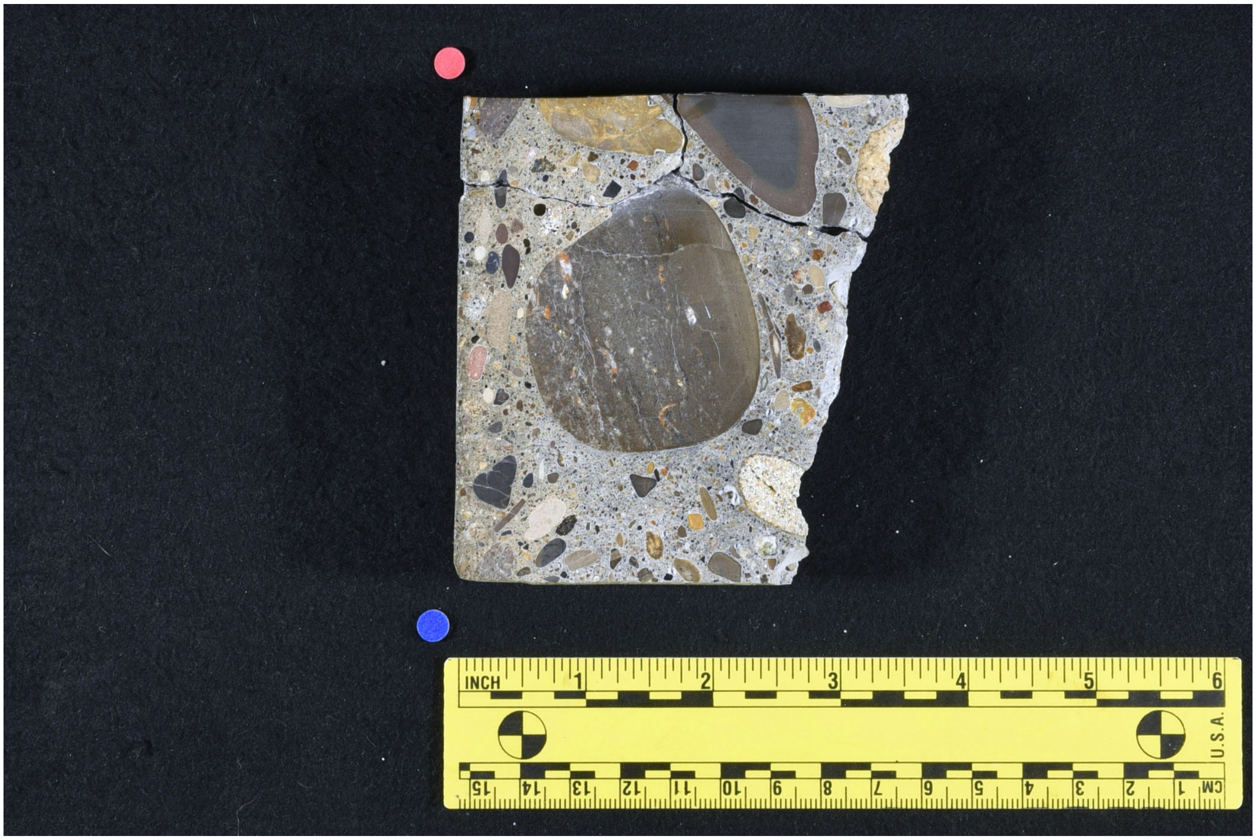

Figure A2. Photographs of the polished surface. The small and large divisions are in centimeters and inches, respectively.

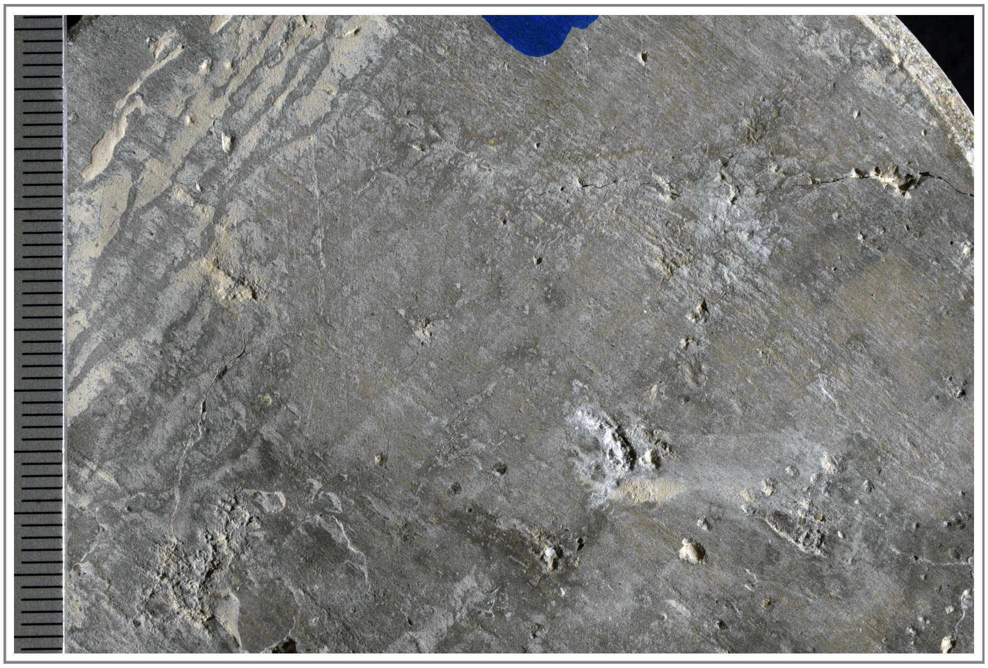

Figure A3. Photograph showing detail of the formed outer surface; scale in millimeters.

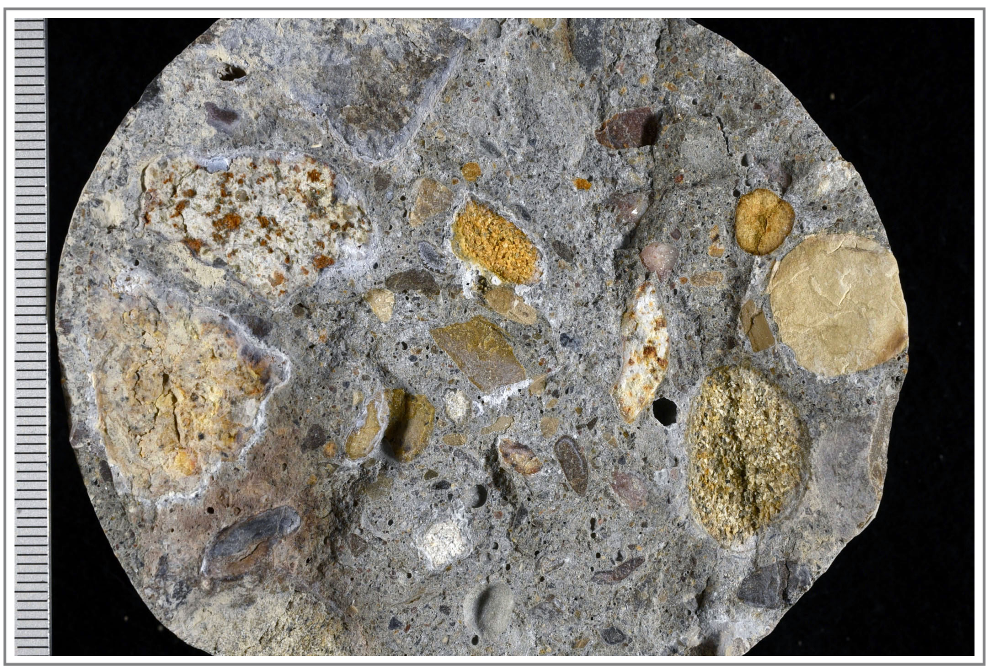

Figure A4. Photograph showing detail of inner fracture surface; scale in millimeters. Note the white deposits of ASR gel on the surface.

(a)

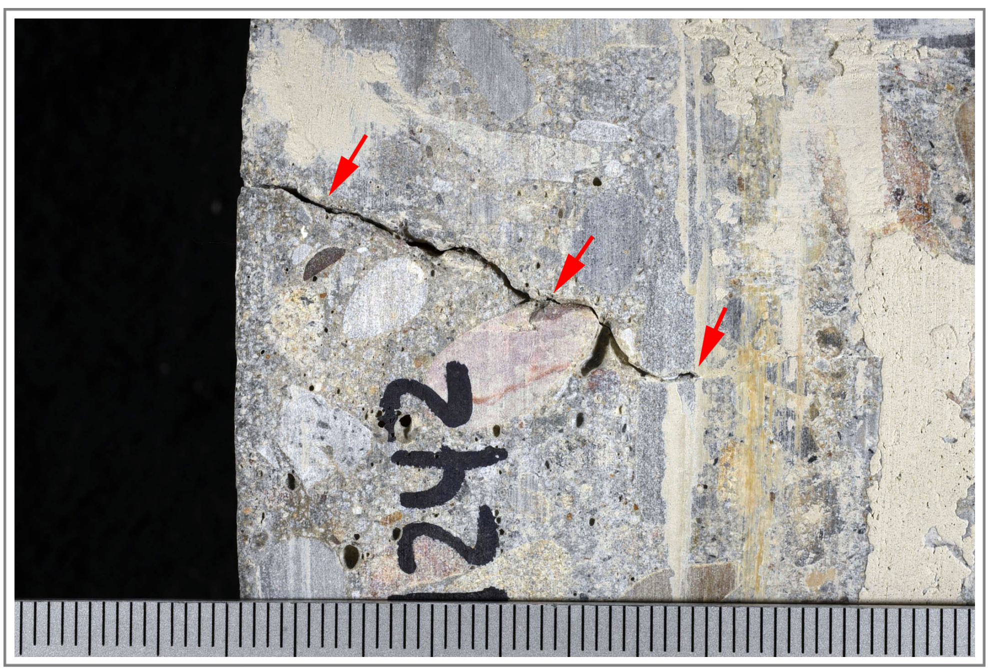

(b)

Figure A5. Photographs of the (a) outer surface and (b) side of the core near the outer surface showing overview of major cracks (red arrows). The scale is in millimeters in both photos.

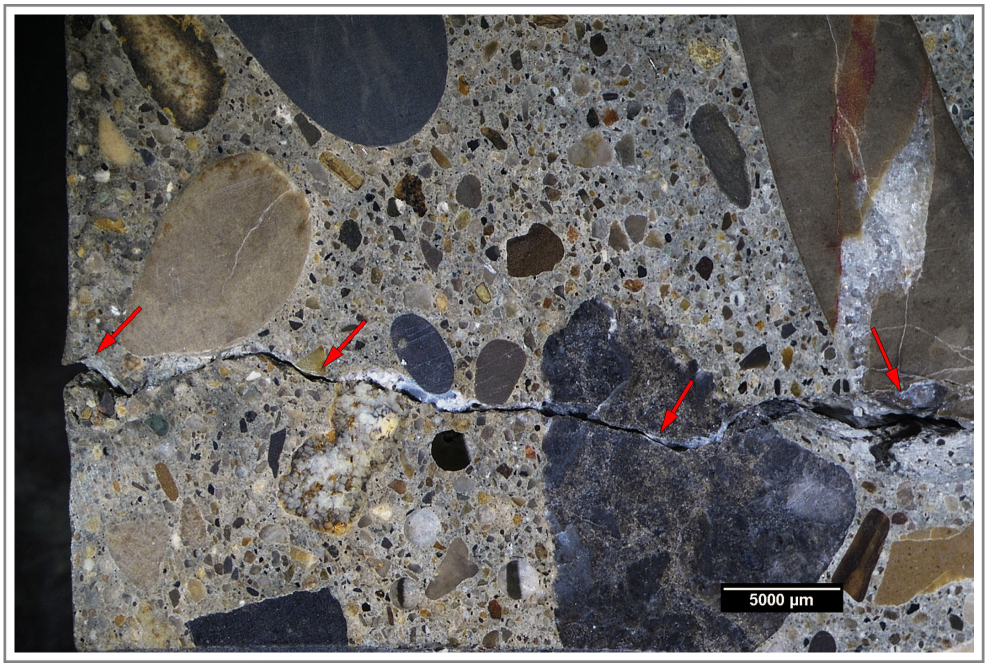

(a)

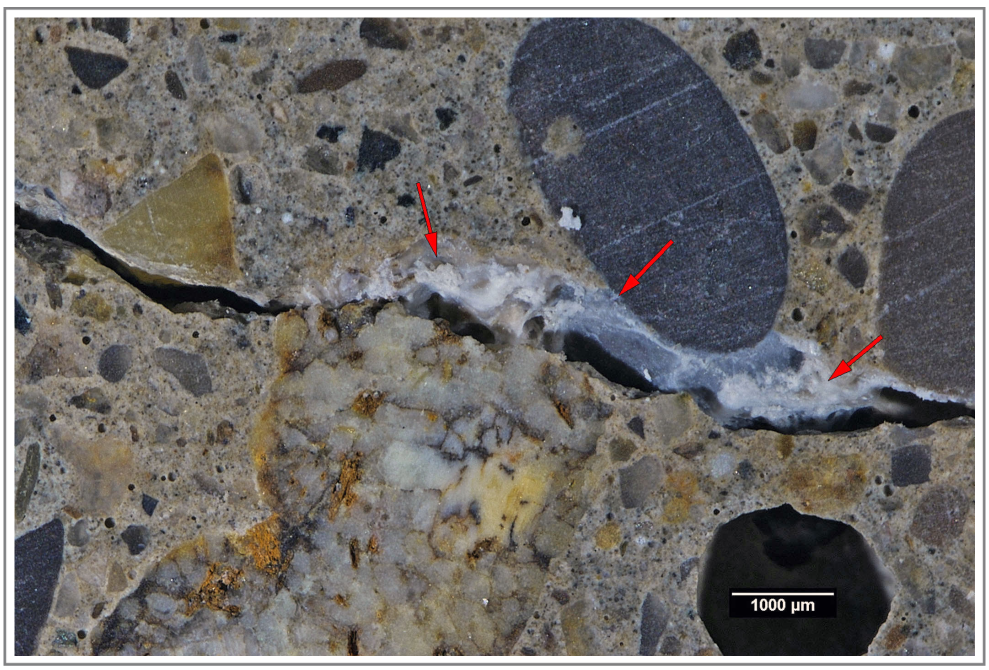

(b)

Figure A6. Reflected light photomicrographs of the polished surface showing (a) overview and (b) detail of main crack (red arrows). The area shown in (b) is ~ 20 mm (¾ in.) from the outer surface. The red arrows in (b) highlight deposits of ASR gel that line the walls of the crack.

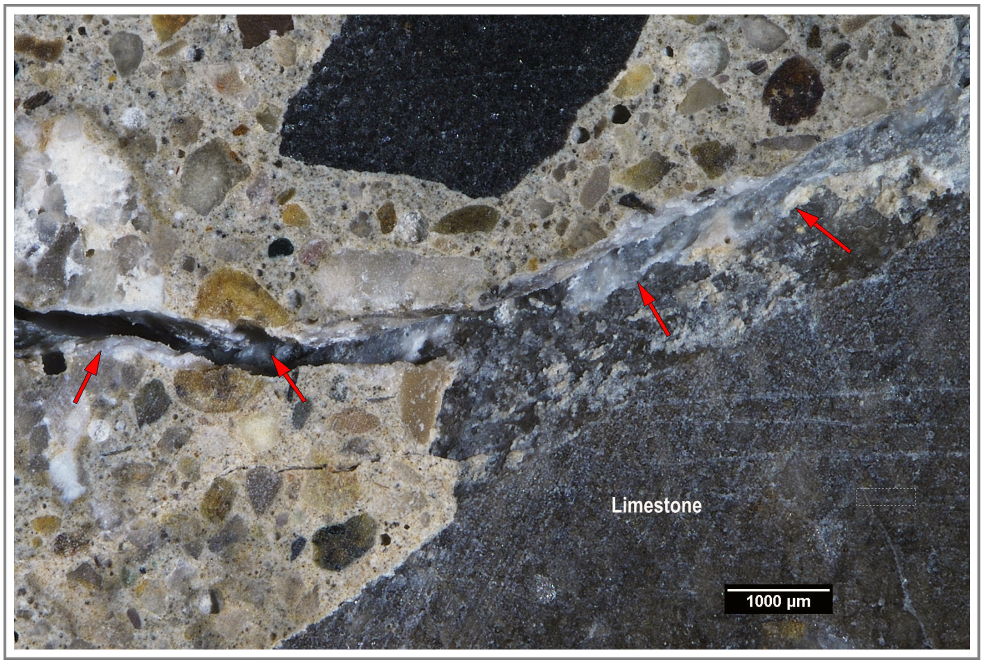

(c)

Figure A6 (cont'd). (c) Reflected light photomicrographs of the polished surface showing detail of main crack about 35 mm (1 ⅜ in.) from the outer surface. The red arrows show deposits of gel lining a particle of limestone along the crack.

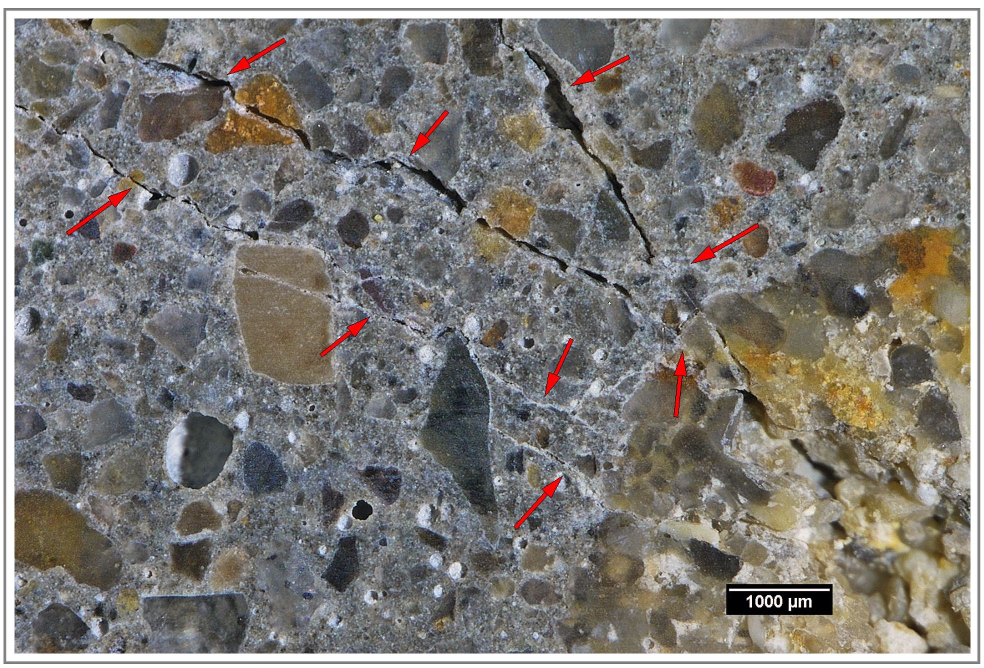

(a)

Figure A7. (a) Reflected light photomicrograph of the polished surface showing detail of microcracks (red arrows) cutting from a quartzite particle into the paste ~ 50 mm (2 in.) from the other surface.

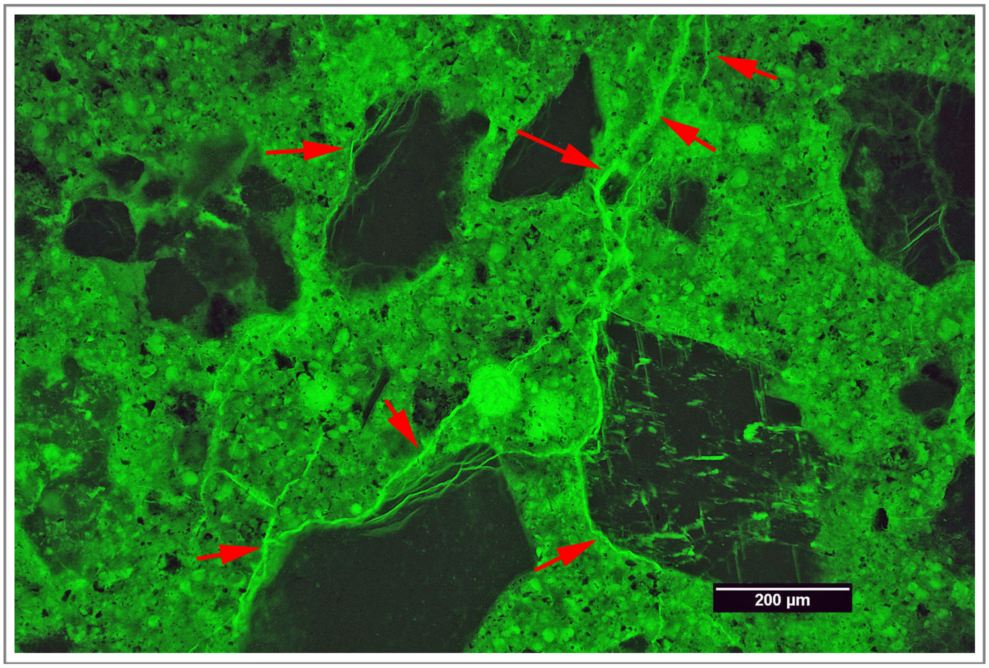

(b)

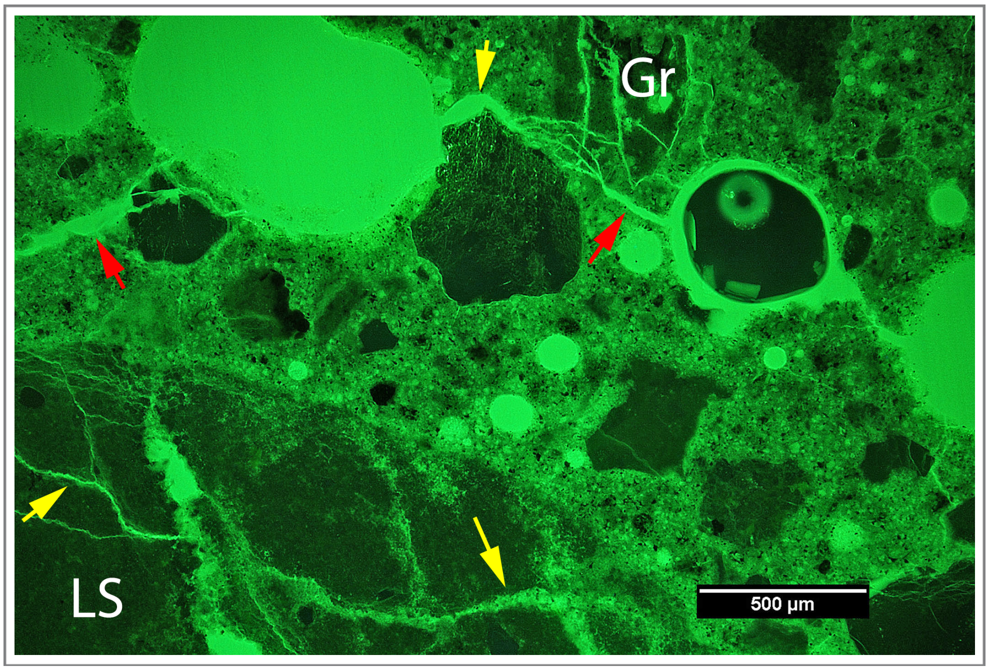

(c)

Figure A7 (cont'd). Transmitted fluorescent light photomicrographs of thin section showing detail of microcracks associated with ASR. In (a) and (b) the red arrows show microcracks cutting through the paste. In (b) the yellow arrows indicate microcracks within a limestone (LS) particle. Gr indicates a granite particle with numerous internal microcracks.

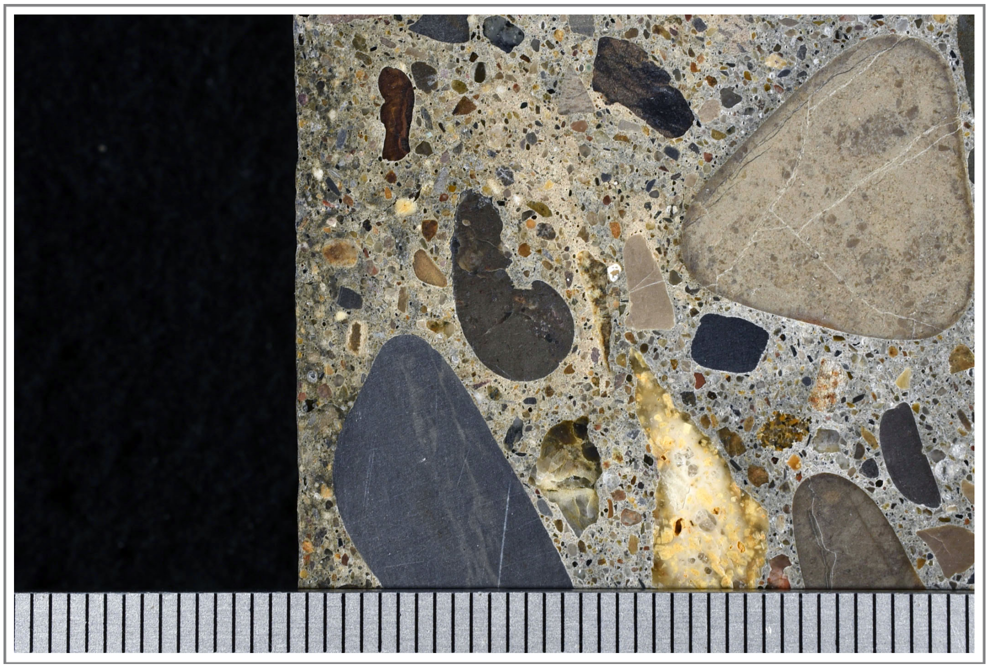

(a)

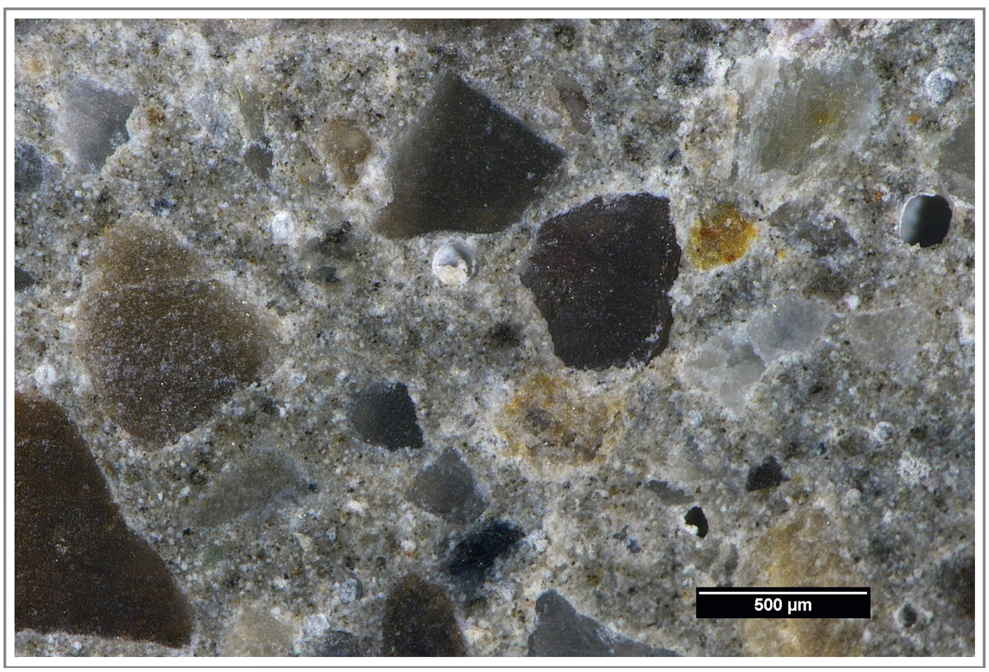

(b)

Figure A8. (a) Photograph of the polished surface showing overview of paste at the outer end of the core; scale in millimeters. (b) Reflected light photomicrograph of the polished surface showing detail of paste in the middle of the core.

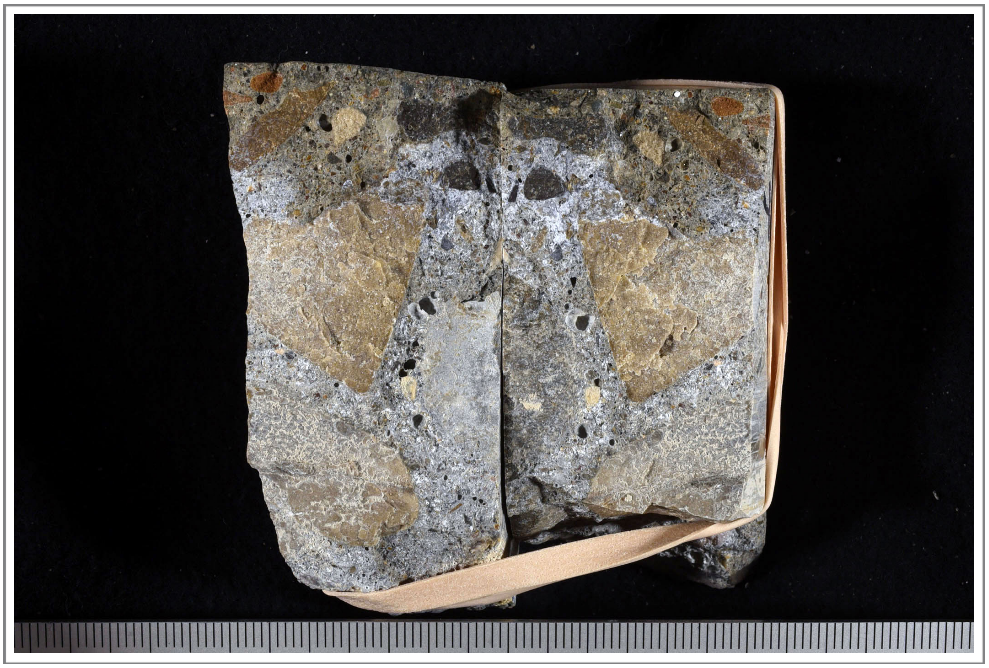

(a)

(b)

Figure A9. Photographs showing (a) overview and (b) detail of fresh fracture surface. The scale is in millimeters in both photos.

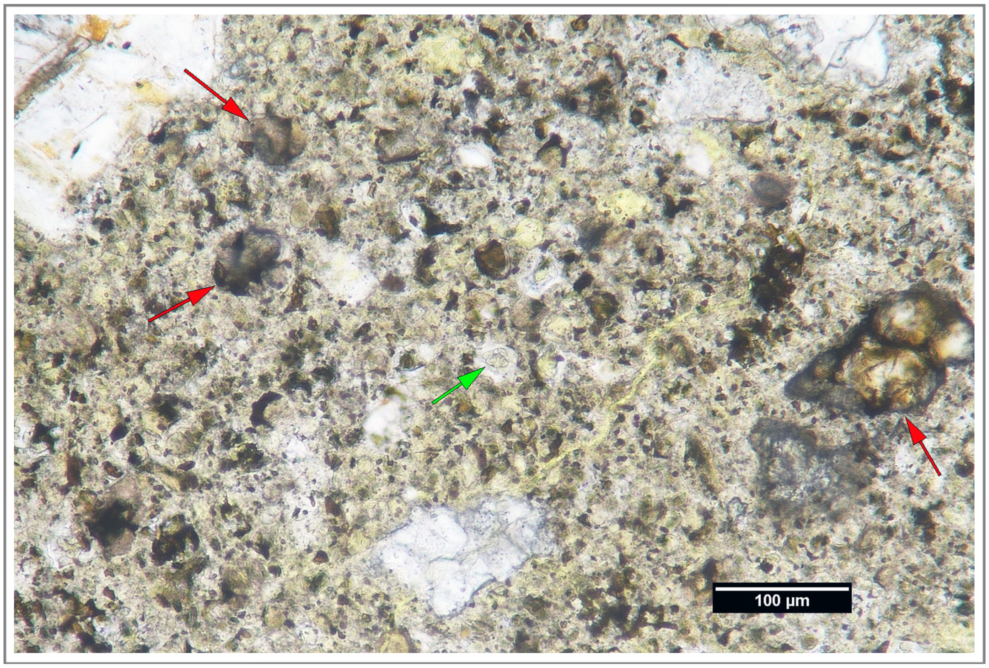

(a)

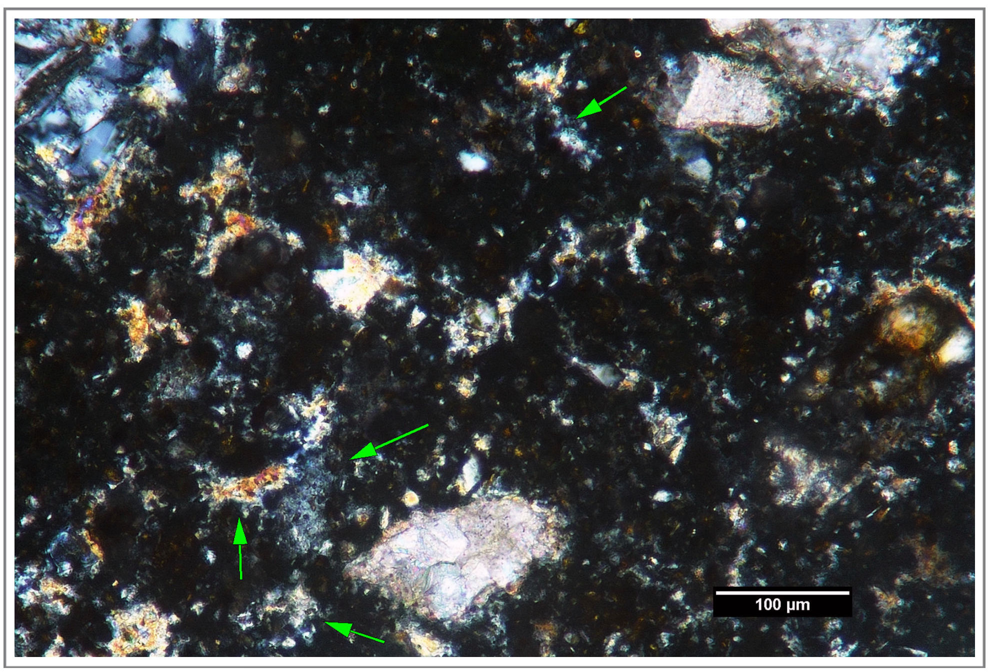

(b)

Figure A10. Transmitted light photomicrographs of thin section showing detail of paste in (a) plane-polarized and (b) cross-polarized light. The red and green arrows in (a) indicate grains of belite and alite, respectively. In (b) the green arrows indicate calcium hydroxide.

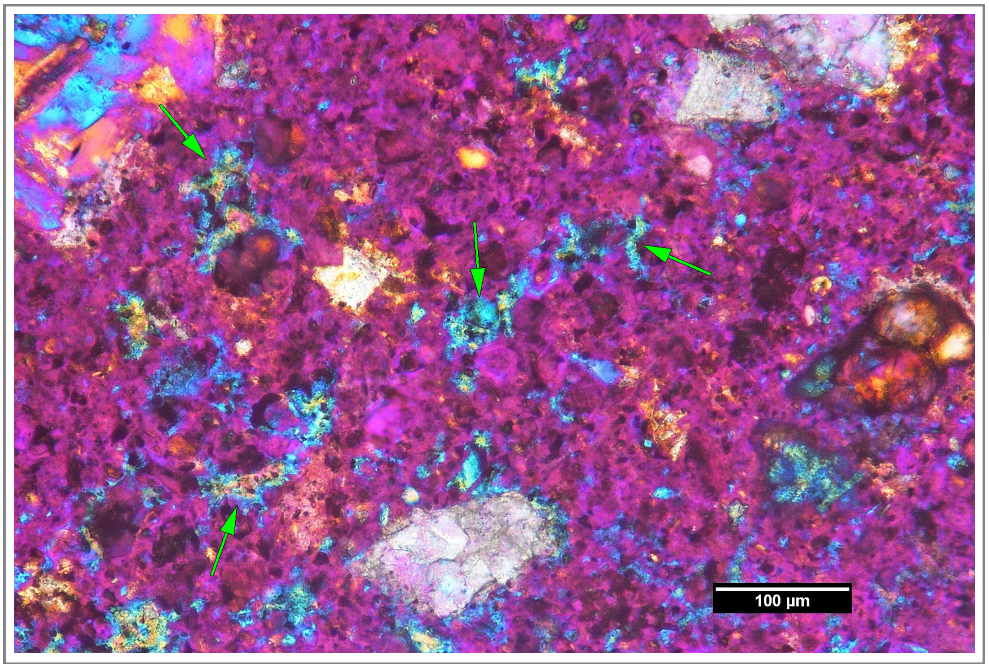

(c)

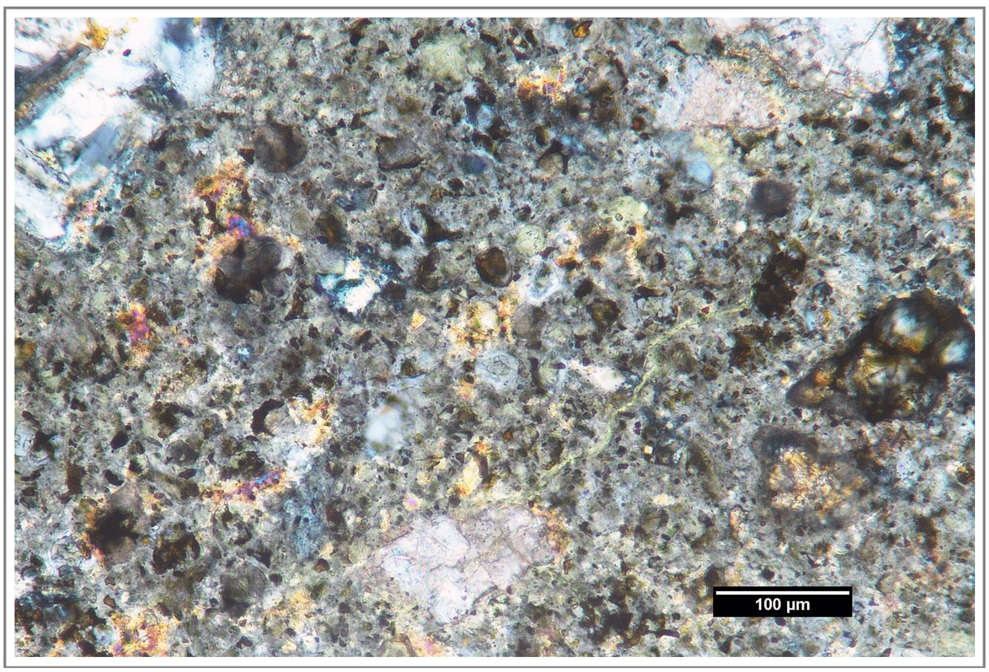

(d)

Figure A10 (cont'd). Transmitted light photomicrographs of thin section showing detail of normally hydrated paste in the middle of the thin section in (c) cross-polarized light with the gypsum plate inserted and (d) cross-polarized light with the quarter wavelength plate inserted. In (c) the green arrows indicate calcium hydroxide.

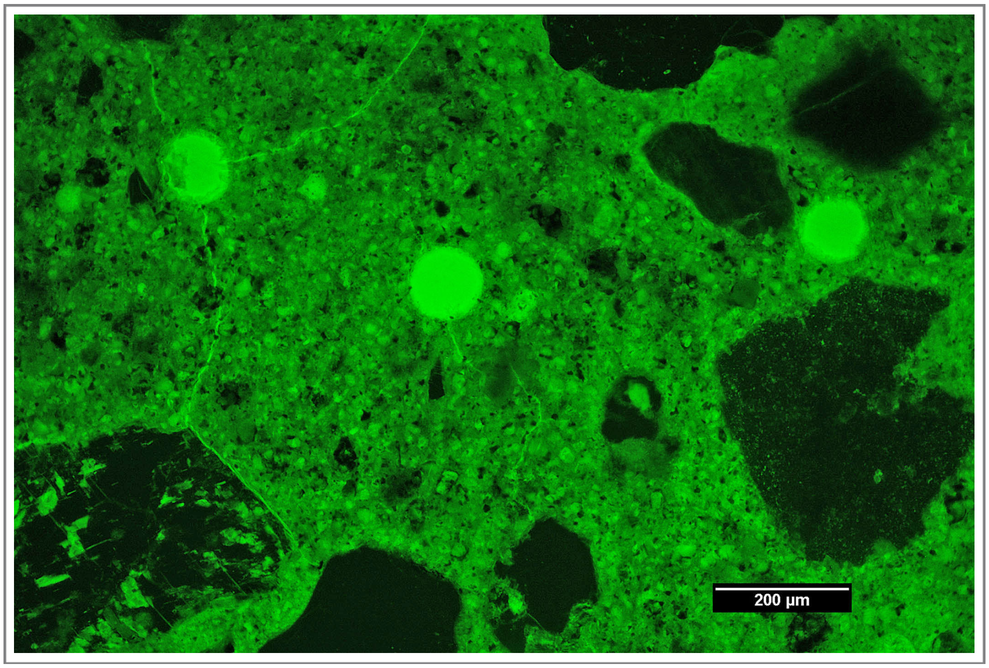

(a)

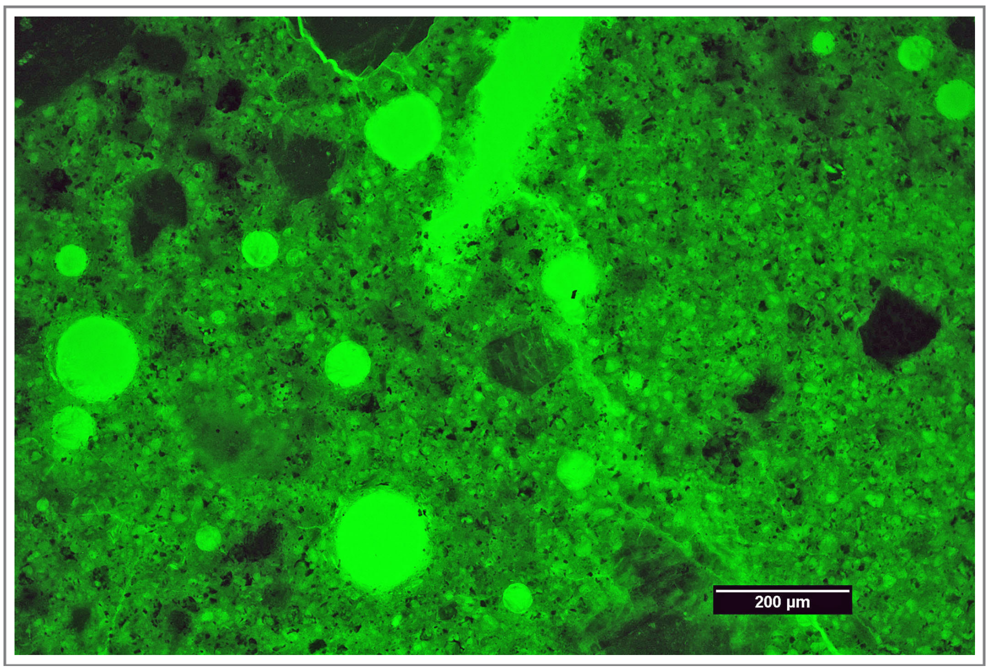

(b)

Figure A11. Transmitted fluorescent light photomicrographs of thin section showing detail of paste in the middle of the thin section. The black areas correspond to aggregate that has very low or effectively zero percent porosity and the bright green circles are air voids filled with epoxy that have 100% porosity. The variations in green between these end members reflect variations in the capillary porosity or micro-density of the paste.

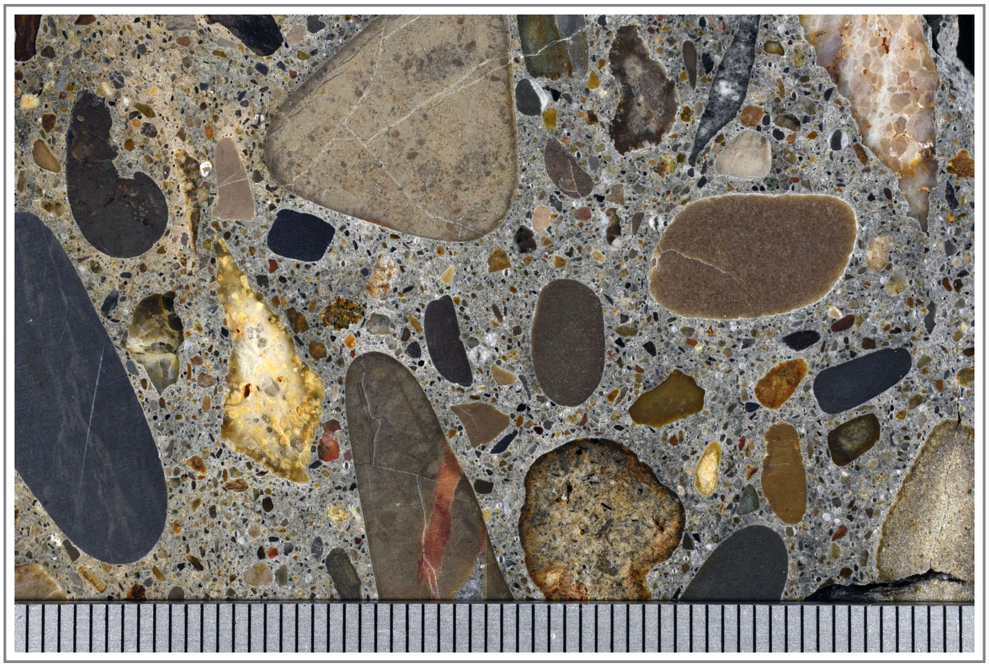

Figure A12. Photograph of the polished surface showing overview of the coarse aggregate in the core; scale in millimeters.

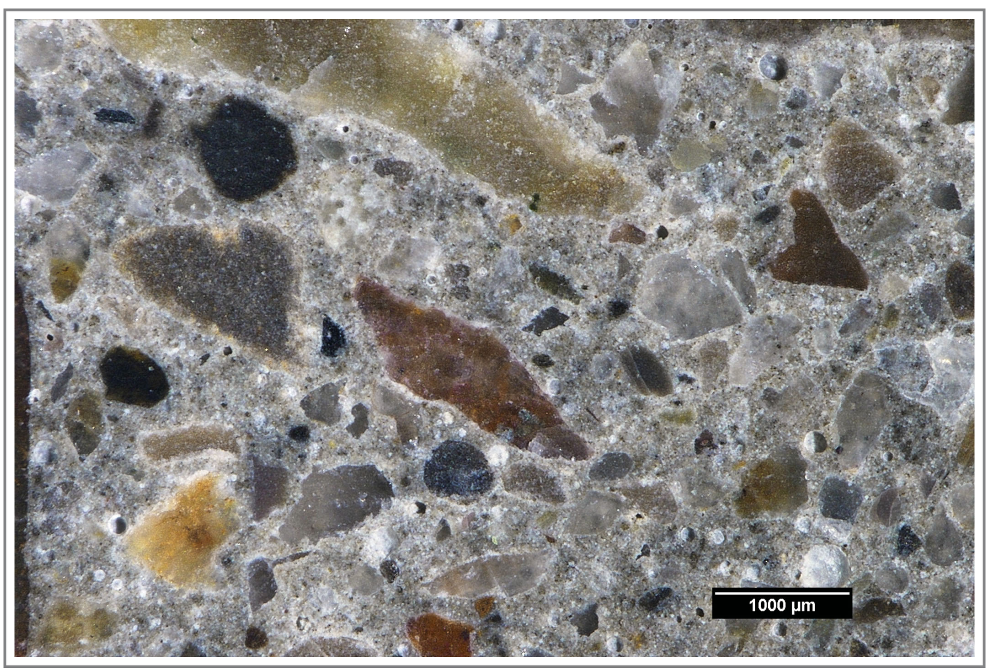

Figure A13. Reflected light photomicrograph of the polished surface showing fine aggregate in the core.

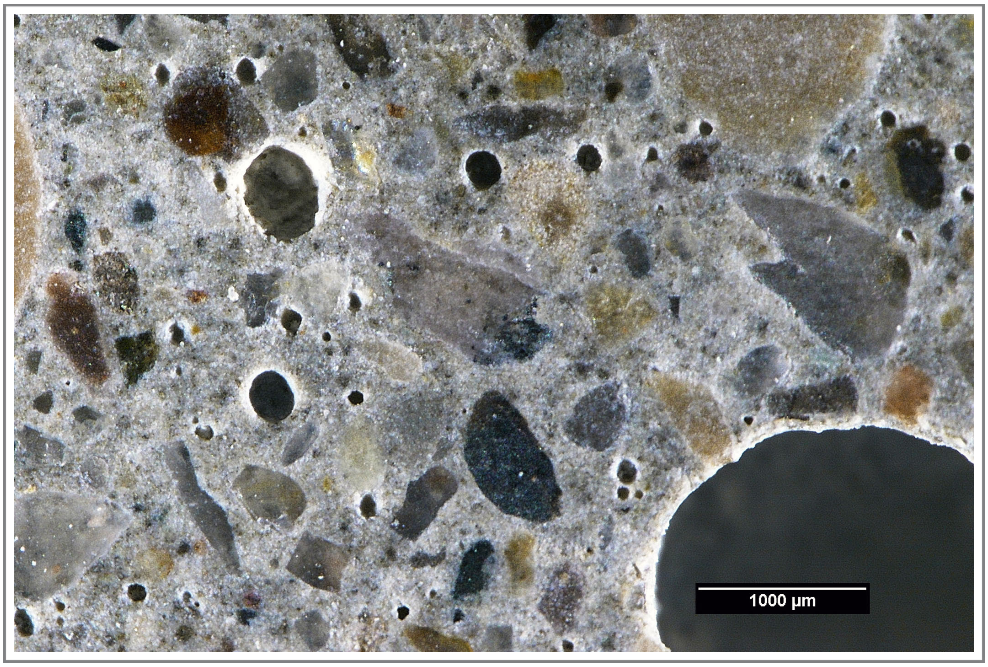

(a)

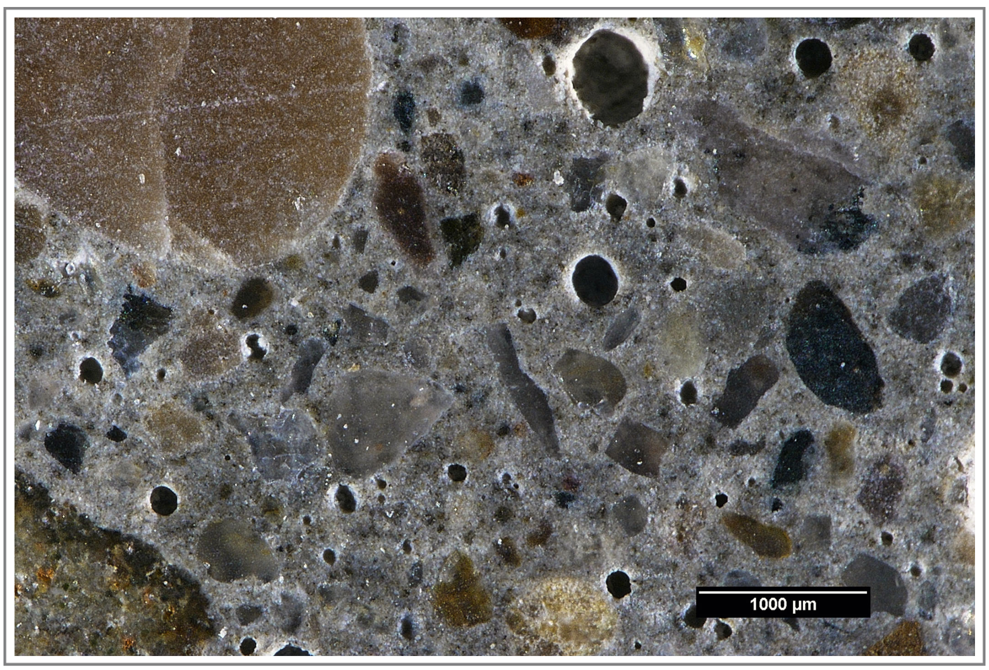

(b)

Figure A14. Reflected light photomicrographs of the polished surface showing air voids (dark circles).

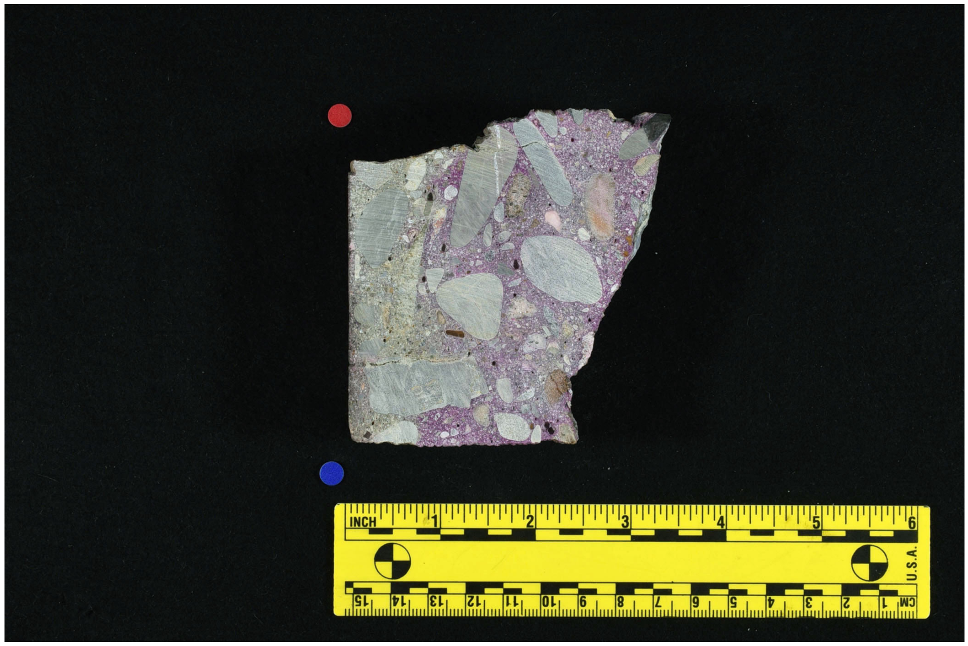

(a)

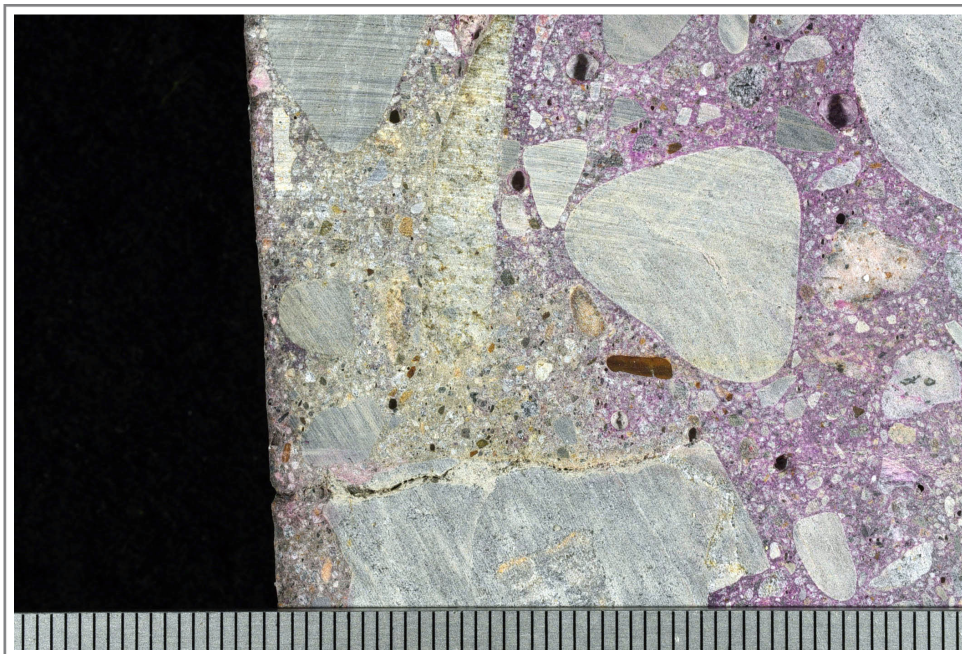

(b)

Figure A15. Photographs showing (a) overview of phenolphthalein-stained surface and (b) detail of surface near the outer surface of the core. The yellow scale in (a) is ~ 150 mm (6 in.) long; the small and large divisions are in centimeters and inches, respectively. The scale in (b) is in millimeters.

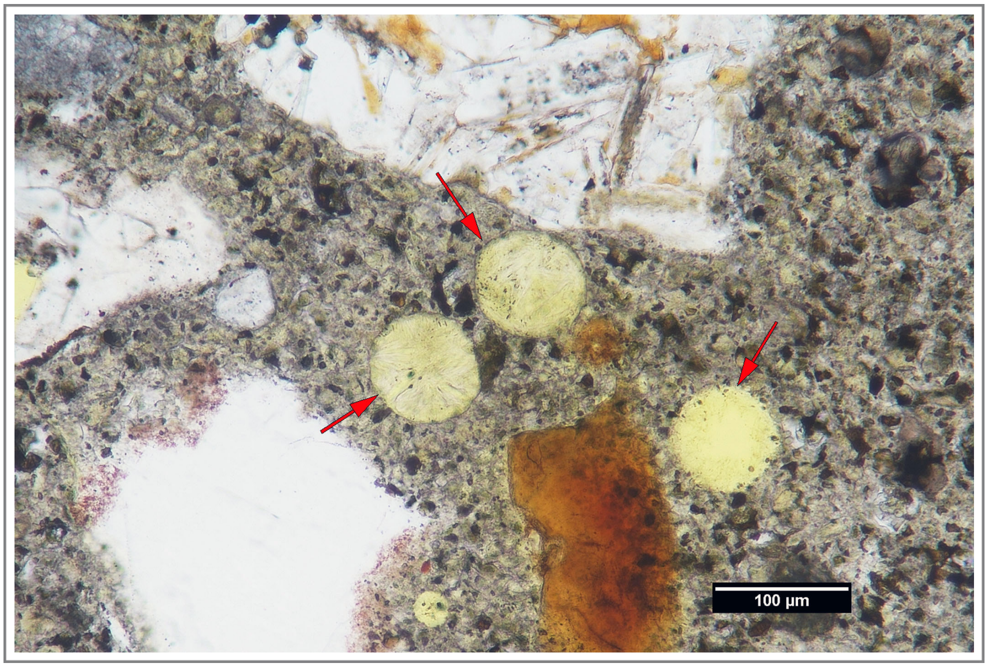

(a)

(b)

Figure A16. Transmitted light photomicrographs of thin section showing deposits of ettringite in voids (arrows) in (a) plane-polarized light and (b) cross-polarized light with the gypsum plate inserted.

(a)

(b)

Figure A17. Photographs of the inner fracture surface showing detail of gel deposits around aggregate particles. Scale in millimeters in both photographs.

PROCEDURES

ASTM C856--Petrographic Analysis The petrographic work was done following ASTM C856 [**1**] with sample preparation done at **DRP** in the following manner. After writing the unique **DRP** sample number on each sample near the received label, the samples were measured and inspected visually and with a hand lens. The orientation of the saw cuts used to prepare the samples was then indicated on each sample with blue and red dots. The samples were then photographed in their as-received condition.

A slab representing a longitudinal cross section of each sample was cut from the central portion of the core using a Raimondini Zipper-105®, a 14-inch diameter water-cooled saw. This produced three (3) longitudinal sections for each core. These sections were rinsed and oven dried in a Gilson® Bench Top laboratory oven at ~ 40°C (~ 105°F). After drying, each piece was labelled with the appropriate **DRP** sample number. One piece was set aside for phenolphthalein staining and the other was set aside for thin section preparation.

The central slab was then lapped and polished on a Diamond Pacific® RL-18 Flat Lap machine. This machine employs an 18-inch diameter cast iron plate onto which Diamond Pacific® Magnetic Nova Lap discs with progressively finer grits are fixed. The Nova Lap discs consist of a $^{1}/_{16}$ in. backing of solid rubber containing magnetized iron particles that is coated with a proprietary Nova resin-bond formula embedded with industrial diamonds of specific grit. The slab preparation involved the use of progressively finer wheels to a 3000 grit (~4 μm) final polish following procedures outlined in ASTM C457 [**2**]. An aqueous lubricant is used in the lapping and polishing process. The polished slab from each sample was examined visually and with a Nikon® SMZ-25 stereomicroscope with 3-158x magnification capability following to the standard practice set forth in ASTM C856.

Phenolphthalein was applied to a freshly saw-cut surface from each sample to assess the extent of carbonation, along with thin section analysis. Phenolphthalein is an organic stain that colors materials with pH of greater than or equal to ~ 9.5 purple. Portland cement concrete generally has a pH of ~ 12.5. Carbonation lowers the pH of the paste below 9.5, so areas not stained by phenolphthalein are an indicator of carbonation. The depth of paste not stained by phenolphthalein was measured from each exposed surface.

1 *Standard Practice for Petrographic Examination of Hardened Concrete.* Annual Book of ASTM Standards, Vol. 4.02., ASTM C856-20.

2 *Standard Test Method for Microscopical Determination of Parameters of the Air-Void System in Hardened Concrete*, Annual Book of ASTM Standards, Vol. 4.02, ASTM C457-16.

Petrographic thin sections were prepared by cutting billets from the remaining longitudinal sections. Outlines marking the area of the billets were drawn with a marker on the saw-cut surfaces after visual and microscopical examination of saw-cut and polished surfaces. The billets were labeled with the unique **DRP** number assigned to the sample then fixed to reference glass with a clear ultra-violet light-activated glue. After the glue hardened, the billets were trimmed and then fixed to a slide with a clear UV activated glue. The billets were then ground and and impregnated with an epoxy that contained fluorescent dye. The impregnated billet was then ground and polished to a thickness of 20-25 µm using a PELCON® automatic thin section machine. The thin section was examined with a Nikon® E-Pol 600 petrographic microscope equipped to provide a 20-1000x magnification range following the standard practice set forth in ASTM C856.

W/CM & Capillary Porosity Estimation Estimation of the w/cm of the paste is obtained from consideration of the color, texture and luster of the paste observed in reflected light, the hardness (Mohs) of the paste measured using calibrated probes, the packing of cementitious materials and the size and abundance of calcium hydroxide observed in plane and cross-polarized transmitted light, and the green tone of images obtained using fluorescence microscopy as described in Nordtest NT Build 361 [**3**]. In cases where pervasive carbonation occurs, the original w/cm cannot be estimated quantitatively. Image analysis methods of photomicrographs obtained in transmitted fluorescent light are then used to obtain quantitative measurements of the relative capillary porosity of the paste in such samples.

3 *Concrete, Hardened: Water-Cement Ratio,* Nordtest Method NT Build 361, Edition 2, 1999